Multiple-Rotor-Cycle 2D PASS Experiments with Applications to ^{207}Pb NMR Spectroscopy

Frederick G. Vogt, James M. Gibson, David J. Aurentz,[1] Karl T. Mueller, and Alan J. Benesi[2]

Department of Chemistry, The Pennsylvania State University, 152 Davey Laboratory, University Park, Pennsylvania 16802-6300

The two-dimensional phase-adjusted spinning sidebands (2D PASS) experiment is a useful technique for simplifying magic-angle spinning (MAS) NMR spectra that contain overlapping or complicated spinning sideband manifolds. The pulse sequence separates spinning sidebands by their order in a two-dimensional experiment. The result is an isotropic/anisotropic correlation experiment, in which a sheared projection of the 2D spectrum effectively yields an isotropic spectrum with no sidebands. The original 2D PASS experiment works best at lower MAS speeds (1–5 kHz). At higher spinning speeds (8–12 kHz) the experiment requires higher RF power levels so that the pulses do not overlap. In the case of nuclei such as ^{207}Pb, a large chemical shift anisotropy often yields too many spinning sidebands to be handled by a reasonable 2D PASS experiment unless higher spinning speeds are used. Performing the experiment at these speeds requires fewer 2D rows and a correspondingly shorter experimental time. Therefore, we have implemented PASS pulse sequences that occupy multiple MAS rotor cycles, thereby avoiding pulse overlap. These multiple-rotor-cycle 2D PASS sequences are intended for use in high-speed MAS situations such as those required by ^{207}Pb. A version of the multiple-rotor-cycle 2D PASS sequence that uses composite pulses to suppress spectral artifacts is also presented. These sequences are demonstrated on ^{207}Pb test samples, including lead zirconate, a perovskite-phase compound that is representative of a large class of interesting materials. © 2000 Academic Press

Key Words: solid-state NMR; ^{207}Pb NMR; magic-angle spinning; 2D PASS; lead zirconate; composite pulses.

INTRODUCTION

Magic-angle spinning (MAS) is commonly applied to obtain high-resolution NMR spectra of spin-$\frac{1}{2}$ nuclei in solids (*1–3*). In some cases, MAS can be used to remove the anisotropic chemical shift interaction, yielding a spectrum containing resonances at their isotropic chemical shifts. More frequently, the anisotropy of the chemical shift interaction is too great for MAS to completely average away, and a manifold of spinning sidebands is produced (*4, 5*). Although they complicate spectra, the spinning sidebands also contain useful information

about the chemical shift tensor (*4, 5*). However, the sidebands from multiple chemical sites can overlap and obfuscate the spectra, rendering any meaningful interpretation difficult or impossible. The 2D PASS (two-dimensional *p*hase-*a*djusted *s*pinning *s*idebands) experiment can overcome this problem, since it separates spinning sidebands by order into individual rows of a 2D NMR experiment (*6, 7*). The information about the anisotropic interaction is then retained, and a quantitative, purely isotropic spectrum can be reconstructed via a shearing transformation and summation of the rows of the data set (*7*). Because the sheared isotropic spectrum no longer contains spinning sidebands but still retains quantitative information, it is often referred to as the "infinite spinning rate" spectrum. The final result of a 2D PASS experiment is an isotropic/anisotropic chemical shift correlation map, which through its second dimension provides additional information on the environment of nuclear sites. Several different forms of the 2D PASS experiment have been successfully applied to a wide variety of materials (*8–12*), including materials containing the ^{207}Pb nucleus (*12*).

Recently, there has been a resurgence in solid-state ^{207}Pb NMR spectroscopy. The ^{207}Pb nucleus has many properties beneficial to its study by NMR spectroscopy, such as a nuclear spin of $\frac{1}{2}$, a reasonable natural abundance (22.6%), and a fairly high resonance frequency (about $\frac{1}{5}$ of that of ^{1}H). Its main drawback as an NMR nucleus is due to its large number of electrons, whose polarizability can lead to a large chemical shift anisotropy (CSA). This in turn produces broad static NMR lineshapes and complicated spinning sideband patterns under MAS. In cases where there is a large deviation from spherical symmetry, the size of the chemical shift anisotropy can exceed several thousand parts per million, as was seen in early ^{207}Pb studies (*13–15*). For the same reasons, the ^{207}Pb nucleus can experience isotropic chemical shifts that range over about 16,000 ppm. Despite these drawbacks, interest in ^{207}Pb NMR has remained high. Recently, there has been an increase in the understanding of the chemical shift parameters in many lead-containing compounds, and significant empirical correlations between ^{207}Pb chemical shift and structure can now be made (*16*). The presence of lead in many types of materials has lead to continuing interest in its characterization

---

[1] Present address: Air Products and Chemicals, 7201 Hamilton Blvd., Allentown, PA 18195-1501.

[2] To whom correspondence should be addressed.

by [207]Pb NMR. Some examples include inorganic salts (13–20) (some of which are environmentally important) and Pb-containing glasses (12, 21–24). Lead is also found in the interesting class of compounds known as perovskite double oxides (25–28). These compounds have generated some interest because of their ferroelectric, antiferroelectric, and piezoelectric properties. [207]Pb NMR in the solid state has just recently been applied to the characterization of these materials (18, 27, 28).

[207]Pb is an ideal candidate for an experiment that correlates isotropic and anisotropic chemical shifts, such as 2D PASS. The anisotropic chemical shift can provide additional site resolution in amorphous materials, in addition to more complete information about the chemical shift tensor. This was convincingly demonstrated for lead phosphate glasses in a recent publication (12). Furthermore, the 2D PASS sequence circumvents the sideband overlap problem that is common in [207]Pb MAS NMR, and generates isotropic [207]Pb spectra that might otherwise be unattainable with the maximum spinning speeds of currently available MAS probes (12). However, fairly fast spinning speeds (around 8–12 kHz) are desirable for 2D PASS on [207]Pb samples, since this reduces the number of 2D rows that need to be acquired, and thus shortens the total experimental time. The spinning speeds needed are attainable with many commercially available MAS probes in the 4- to 6-mm rotor diameter range. Unfortunately, the single-rotor-cycle PASS sequences currently available are designed for lower spinning speeds, and finite pulse widths can lead to "collisions" between pulses at higher spinning speeds, such as those required for [207]Pb PASS.

In this paper, we extend the 2D PASS experiment to multiple rotor periods, making it easier to apply at higher spinning speeds. Multiple-rotor-cycle extensions were recently applied to the closely related quadrupolar PASS (QPASS) experiment (29), which separates quadrupolar sidebands by their order (30). The extra time provided by multiple rotor cycles also allows for the incorporation of composite π pulses (31) in the PASS sequence, as was previously demonstrated for both 1D PASS (10) and for the 1D *to*tal *s*uppression of *s*idebands (TOSS) sequence (32). This is primarily of interest for [207]Pb samples with longer spin–spin relaxation (T_2) values, where the sharper peaks can often enhance artifacts in PASS spectra that arise due to the poor B_1 homogeneity and excitation bandwidth of RF pulses. The use of composite π pulses, which correct for these nonidealities, is shown to greatly alleviate this problem. The pulse sequences are demonstrated on lead-containing samples, including perovskite-phase lead zirconate (PbZrO$_3$).

MULTIPLE-ROTOR-CYCLE 2D PASS SEQUENCES

The 2D PASS experiment has recently been analyzed theoretically using general symmetry arguments, and the sequence has been specified in terms of "PASS equations" that give the positions of RF pulses within the sequence (7, 33). In the analysis, many simplifications and insights are obtained by the development of the "carousel" concept (34). Chemically equivalent powder sample sites are members of a carousel if they have the same values for the angles α_{PR} and β_{PR}, two of the three angles that relate the CSA tensor in its principal axis system to the MAS rotor axis system (7, 33, 34). The third angle, γ_{PR}, is different for the sites in the carousel, and its powder average is the basis of the ability of PASS sequences to phase shift an MAS sideband of order k by the "pitch" angle Θ (6, 7, 33). The carousel allows for the derivation of sideband amplitude and phase behavior without inclusion of the angles α_{PR} and β_{PR}. The 2D PASS experiment is unlike most conventional 2D NMR experiments in that its second dimension is specified by the pitch angle. This can be seen from the complex amplitude of a sideband under a PASS sequence of pitch Θ, which is shown in Ref. (7) to be given by

$$a^{\Theta(k)} = a^{0(k)}\exp(-ik\Theta)\exp(-\lambda T). \quad [1]$$

Here $a^{0(k)}$ is the complex spinning sideband amplitude in a normal MAS spectrum, T is the total duration of the PASS sequence, and λ represents a relaxation decay constant that will be discussed further below. The pitch Θ is incremented from 0 to 2π to form the second dimension in a 2D PASS experiment. Equation [1] indicates that pitches of $\Theta = 0$ and $\Theta = 2\pi$ represent no phase shift of any sidebands (i.e., like an ordinary MAS spectrum), while other values of Θ lead to spectra containing sidebands that are phase shifted by an angle of $-k\Theta$. The additional relaxation decay in Eq. [1] also indicates that the effects of relaxation can lead to a variable linewidth in the pitch dimension of a 2D PASS experiment if the duration of the sequence varies with Θ, thus yielding undesired interference between the rows of the 2D experiment. Constant-duration 2D PASS sequences avoid this problem, and are the only type of sequence discussed in the present work (7).

Actual 2D PASS pulse sequences can be designed by solving the "PASS equations," which are reproduced below (7):

$$2 \sum_{q=1}^{n} (-1)^q \exp[im\theta_q] + 1 - (-1)^n \exp[im(\Theta + \theta_T)] = 0 \quad [2]$$

$$(-2) \sum_{q=1}^{n} (-1)^{n+q}\theta_q + \theta_T = 0. \quad [3]$$

In Eqs. [2] and [3], θ_q represents the timing of the qth pulse given as an angle (i.e., $\theta_q = \omega_r \tau_q$ where τ_q is the timing of the qth pulse), n is the number of pulses in the PASS sequence, and θ_T is the total duration of the sequence expressed as an angle (for one- or multiple-rotor-cycle PASS, $\theta_T = 2\pi, 4\pi, 6\pi$, or higher integer multiples of 2π). The variable m in Eq. [2] results from the Fourier expansion of the time dependence of

the chemical shift Hamiltonian under MAS, and requires that Eq. [2] be expanded into two equations, one for $m = 1$ and one for $m = 2$ (35). For half-integer quadrupolar nuclei, the time dependence of the MAS second-order Hamiltonian requires that the range of m be extended from 1 to 4, as is done in the QPASS experiment (30). The first PASS equation contains the requirement for sideband phase shifting as shown in Eq. [1]. The second PASS equation imposes an additional constraint, known as the Hahn echo condition, so that the pulse sequence introduces no additional phase shifts via the isotropic chemical shift (33). Equation [2] yields four equations when it is expanded into $m = 1$ and 2 with separate real and imaginary parts, which are combined with Eq. [3] to yield five nonlinear equations with n unknowns. These equations were solved in previous work for $\theta_T = 2\pi$, which we refer to as the one-rotor-cycle solution. This solution is the successful five-pulse, constant-duration, single-rotor-cycle 2D PASS sequence that was first proposed in Ref. (7), and was demonstrated for ^{13}C in both oriented and powder samples (9, 11), typically at slower MAS speeds in the range 1–3 kHz.

The major problem with performing the five-pulse, constant-duration 2D PASS experiment at higher spinning speeds is the possibility of overlap of the five π pulses. An example would be an attempt at 2D PASS at a 12-kHz spinning speed, where the rotor period is just 83.3 μs in duration. Using the PASS timings given by Antzutkin et al. (7), and used for high-speed 2D PASS on ^{207}Pb by Fayon et al. (12), one finds a minimum pulse spacing of 0.07687 rotor revolution (between the second and third pulses), or 6.4 μs. (The use of a shifted echo in Ref. (12), discussed below, alleviates a similar pulse spacing problem between the fourth and fifth pulses). Therefore, if the probe or spectrometer cannot achieve a RF power of at least 78 kHz, so that the π pulses are less than 6.4 μs in duration, the experiment cannot be performed at this spinning speed. Unfortunately, as previously noted, high spinning speeds are very desirable for ^{207}Pb 2D PASS experiments, since a smaller number of pitch angles leads to shorter overall experimental times. Since many commercial MAS probes, especially those using 5- and 6-mm rotors, are incapable of achieving this RF power, many users are left with a dilemma when attempting to implement PASS experiments on nuclei like ^{207}Pb.

A solution to this problem is the use of a multiple-rotor-cycle PASS experiment. Such an experiment is shown in Fig. 1, for the case of a two-rotor-cycle experiment. The shifted-echo version of the sequence is shown, in which additional delays of one rotor cycle are inserted prior to and after the last pulse so that echo detection is possible (6, 12). As long as fairly well-spaced solutions to the PASS equations can be found for two rotor cycles, the sequence will relieve the stringent requirement on probe RF power. These solutions to the PASS equations for multiple rotor cycles can in fact be found via a method similar to that used for the QPASS experiment (29). The equations are solved via a Newton–Raphson method with random starting points and the multiple solutions returned
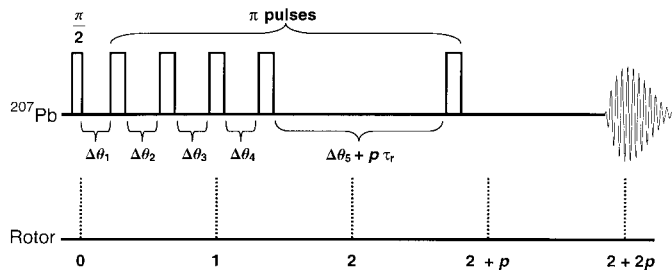

FIG. 1. A five-pulse, 2D PASS sequence for ^{207}Pb NMR with two rotor cycles of evolution. The shifted-echo version is depicted (see text). Normally, p is set to 1 to minimize relaxation effects. The lengths of the delays $\Delta\theta_1$ to $\Delta\theta_5$ are determined by the solution set used for a particular pitch in the PASS experiment, and are the differences between the θ values given in Tables 1 and 2 multiplied by the rotor period.

by this procedure are screened in order to find well-separated delays for each pitch. The *Mathematica* programming environment (36) can be used for such a task, and good solutions can typically be found with about 1–2 days of computer time on PC workstations. Other methods exist for solving equations of this sort, such as Broyden's method (37), but because of the constraint that the solutions must be well spaced, they offer little advantage over the fast and reliable Newton–Raphson method. We also note that the graphical method recently employed in Ref. (10) would also be applicable to this problem, and might show some additional advantages over the method used here.

EXPERIMENTAL

All ^{207}Pb NMR spectra were obtained on a Chemagnetics/Varian Infinity 11.7-T spectrometer operating at spectral frequencies ranging from 104.16 to 104.38 MHz. Experiments were run without a field-frequency lock, as the magnet used has a field drift rate of less than 2.5 Hz per h, which is not sufficient to produce the spectral artifacts discussed in Ref. (11). The experiments were performed using a 5-mm double-resonance Chemagnetics MAS probe (Model MPRB 500318). The spinning rate during all experiments was locked to within ±2 Hz of the set value using a Chemagnetics MAS speed controller (Model M806403000). As the chemical shift of lead compounds is often temperature dependent (38–40), temperatures in the probe sample chamber were held at 23.0 ± 0.1°C via a Chemagnetics variable temperature accessory (Model M806114000). Radiofrequency pulses for the experiments were set to the strongest power available, and pulse widths were in the range of 3–4 μs for $\pi/2$ pulses and ~7 μs for π pulses. The spin–lattice (T_1) relaxation times were obtained for all samples, using either inversion-recovery methods (41) or data already given in the literature, and recycle delays were set accordingly to allow for full relaxation. The lead compounds used in this work are commercially available, and were obtained from Aldrich Chemical Co. All chemical shifts were externally referenced to tetramethyl lead at 0 ppm via a sec-
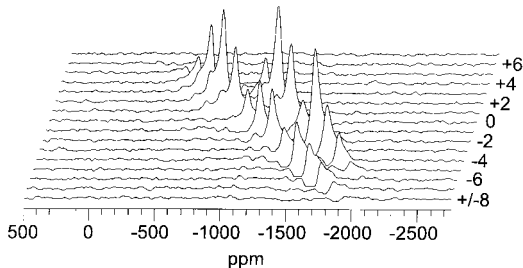
FIG. 2. Results of a two-rotor-cycle 2D PASS experiment on a sample of PbZrO$_3$. The data set was acquired at a spinning speed of 12 kHz, with a π pulse duration of 7.0 μs and a recycle delay of 8 s. For each of the 16 pitches, 972 scans were acquired, using shifted-echo detection (see text or Ref. (12)). An oversampled spectral width of 1.5 MHz was employed to clearly map out the shifted echo. The total 2D experimental time was 35 h. The 243-step phase cycle used in this experiment selects a $(+1) \rightarrow (-1) \rightarrow (+1) \rightarrow (-1) \rightarrow (+1) \rightarrow (-1)$ coherence pathway (see text).

ondary reference (16). The 2D PASS experiments are inherently phase-sensitive in the pitch dimension (see Eq. [1]), so there is no requirement for special 2D phase-sensitive acquisition conditions.

RESULTS AND DISCUSSION

A Two-Rotor-Cycle, Shifted-Echo 2D PASS Experiment

As a demonstration of multiple-rotor-cycle 2D PASS applied to ^{207}Pb NMR, a two-rotor-cycle 2D PASS experiment was performed at a high MAS speed (12 kHz) on a sample of crystalline lead zirconate (PbZrO$_3$). This material exhibits a large CSA, and has two crystallographically distinct lead sites (18, 26). Under MAS at 12 kHz, the spectrum contains 14 detectable sidebands. The results of the two-rotor-cycle 2D PASS experiment are shown as a stacked plot in Fig. 2. Each sideband is separated into a row of the two-dimensional experiment. The pulse timings used in this experiment were calculated as discussed above for $\theta_T = 4\pi$ and are presented in Table 1. The shifted-echo version of the 2D PASS sequence (as shown in Fig. 1) was used because of the breadth of the spectrum (12), so that the timing of the fifth pulse is advanced by a single rotor period (i.e., 83.3 μs).

The T_1 relaxation time of PbZrO$_3$ is approximately 1.5 s, so that a recycle delay of 8 s ensured complete recovery of longitudinal magnetization. Because of this relatively short recycle time, an extended phase cycle for the five π pulses was used in this experiment. Each π pulse is independently phase cycled in steps of $2\pi/3$ to yield a 243-step phase cycle (as in Ref. (7)) that is designed to select a coherence transfer pathway of $(+1) \rightarrow (-1) \rightarrow (+1) \rightarrow (-1) \rightarrow (+1) \rightarrow (-1)$. The receiver phase is calculated from

$$\psi_{\text{receiver}} = 2(\psi_1 - \psi_2 + \psi_3 - \psi_4 + \psi_5), \qquad [4]$$

where ψ_1 through ψ_5 are the phases of the five π pulses. In

addition, simple quadrature phase cycling of the $\pi/2$ pulse (and the receiver) was simultaneously used with the above phase cycle.

The most significant advantage of the two-rotor-cycle 2D PASS experiment is its avoidance of pulse overlap. As mentioned before, at a 12-kHz MAS speed, the π pulses cannot exceed 6.4 μs in duration, or overlap will occur. In our case, we were unable to achieve this power without occasional arcing of the probe coil. With two-rotor-cycle PASS, the minimum pulse spacing becomes 0.10071 rotor revolution, which corresponds to a maximum π pulse width of 8.4 μs (about 60 kHz of RF power). In our case, this reduction in RF power is enough to make the experiment possible without destructive electrical arcing inside the probe.

While reducing the MAS speed could also alleviate the pulse width problem, the use of higher spinning speeds effectively decreases the total experimental duration by requiring fewer 2D rows. In the case of PbZrO$_3$, the use of a 16-pitch experiment at 12 kHz is optimal, as there are just enough 2D rows to hold the 14 discernible sidebands. If the experiment were performed at 10 kHz MAS speed, the sidebands would fold in the second dimension unless more pitches were used. As many spectrometer software packages can only perform the fast Fourier transform on data sets that are 2^n in length, this requirement avoids the use of either a 32-pitch experiment (using the spectrometer software) or additional processing software that performs Fourier transforms on data sets that are not 2^n in length.

A shear transformation (7) can be applied to the 2D PASS data to construct an isotropic/anisotropic correlation spectrum, as is shown in Fig. 3. The isotropic projection of the sheared

TABLE 1
Timings for π Pulses, in Units of Sample Revolutions, for Two-Rotor-Cycle PASS

Pitch ($\Theta/2\pi$)	$\theta_1/2\pi$	$\theta_2/2\pi$	$\theta_3/2\pi$	$\theta_4/2\pi$	$\theta_5/2\pi^a$
0.0000	0.25941	0.75534	1.00000	1.25941	1.75534
0.0625	0.39721	0.74701	1.02130	1.40778	1.73628
0.1250	0.45239	0.82796	1.04547	1.47400	1.80411
0.1875	0.50024	0.90483	1.07523	1.53303	1.86239
0.2500	0.54353	0.97566	1.11202	1.58717	1.90729
0.3125	0.15459	0.63853	0.93986	1.04057	1.58466
0.3750	0.19999	0.68872	0.96387	1.10052	1.62538
0.4375	0.24568	0.73895	0.98300	1.15658	1.66686
0.5000	0.29022	0.79022	1.00000	1.20978	1.70978
0.5625	0.33314	0.84342	1.01700	1.26105	1.75433
0.6250	0.37462	0.89948	1.03613	1.31128	1.80001
0.6875	0.41534	0.95943	1.06014	1.36147	1.84541
0.7500	0.09271	0.41283	0.88798	1.02434	1.45647
0.8125	0.13761	0.46697	0.92477	1.09517	1.49976
0.8750	0.19589	0.52600	0.95453	1.17204	1.54762
0.9375	0.26372	0.59222	0.97870	1.25299	1.60279

^{a} For shifted-echo detection, one or more additional rotor cycles can be inserted prior to and after this delay, as shown in Fig. 1.
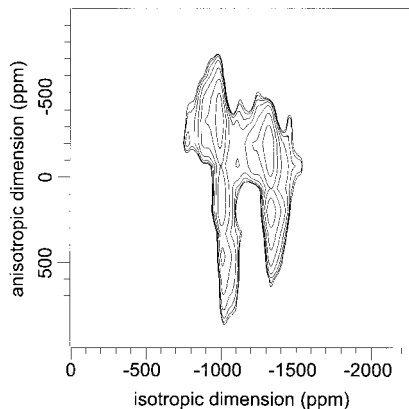
FIG. 3. Results of the two-rotor-cycle 2D PASS experiment on $PbZrO_3$, after the shearing transformation, presented as a contour plot to highlight the isotropic-to-anisotropic correlation and the magnitudes of the CSA for the two sites.

spectrum can be obtained by summation along the vertical axis, and is given, along with the MAS spectrum, in Fig. 4. The two sites expected from the crystal data are clearly visible in the isotropic projection at -1000 and -1349 ppm, and their integrals are very close to a one-to-one ratio, as expected. The analysis of the $PbZrO_3$ spectrum, as far as counting sites and obtaining quantitative information is concerned, is clearly simplified over the MAS spectrum since no changes in spinning speed are required. Because the sites are only 350 ppm apart, only a very high speed MAS probe (>30 kHz) would allow for the sideband separation needed to quantitatively analyze them.

These two sites in $PbZrO_3$ are expected from the crystal analysis, and their presence in NMR spectra has been noted in earlier work (18, 28). However, to our knowledge, the [207]Pb NMR data have not been clearly assigned to the individual lead sites known from the crystal data. The isotropic/anisotropic correlation spectrum in Fig. 3, combined with new data relating [207]Pb chemical shifts to molecular structure (16), allows for tentative assignments to be made. Due to the lattice shift of the lead atoms, the Pb in lead zirconate can be best described as three-coordinate Pb^{2+}, situated in a distorted perovskite structure with an orthorhombic unit cell (26). The crystal data yield an average distance of the two Pb sites (labeled Pb′ and Pb″ in Ref. (26)) to their coordinating oxygens of 2.5646 and 2.4756 Å, respectively. As shorter Pb–O distances have been shown to correlate with higher [207]Pb chemical shifts (16), the resonance at -1000 ppm is likely due to the Pb″ site, and that at -1349 ppm due to the Pb′ site. As is shown by Fayon et al. (16), the correlation between bond length and chemical shift is no longer linear for lower coordination numbers, but the general trend is still correct, making these assignments probable. The general trend in chemical shift values for $PbZrO_3$ also suggests a heightened degree of covalent character in the ionic bonding of lead to its closest oxygen neighbors, relative to other ionic lead compounds (42).

The relative anisotropy of the two sites (Fig. 3) reinforces

the above assignments, as this value has been empirically shown to increase in size with increasing chemical shift for many similar classes of compounds (16, 43). The greater deviation in Pb–O bond length for the Pb″ site also predicts a relatively higher CSA, as was shown in model studies of orthophosphates (43). Due to the extreme width of the spectrum, attempts at extracting the full chemical shift tensors from both the complete set of sideband intensities and a subset of the more intense sidebands have led to poor results. The fact that the sidebands are 12 kHz apart, coupled with the finite (and fairly narrow) excitation bandwidth of the pulse sequence, leads to distortion of nearly all of the sideband intensities. While this is too great to allow for uncorrected fit procedures, the situation can be improved by numerical simulation procedures, if desired, as was done by Neue et al. (17). Other causes of distortion, such as finite probe bandwidth, resonance offset effects, and B_1 inhomogeneity, may also be correctable via numerical methods. For amorphous samples, the relative shape of the CSA pattern is enough to discern different sites and CSA magnitudes, so the full tensor fitting information is not very useful (as a distribution of values is present) and would be unnecessary (12).

The considerations discussed above can also lead to a distortion of the isotropic infinite spinning rate spectrum. The transmitter frequency used in this experiment corresponded to about -1116 ppm on the chemical shift scale used here. This lies at almost the exact center of the MAS spectrum shown in Fig. 4a. We have found that transmitter offsets of ~25 kHz can lead to gradually increasing errors in the quantitative analysis of the isotropic spectrum, and so we recommend both careful placement of the transmitter frequency and multiple experiments at several offset frequencies to ensure quantitative accuracy for unknown samples. The quantitative accuracy ob-
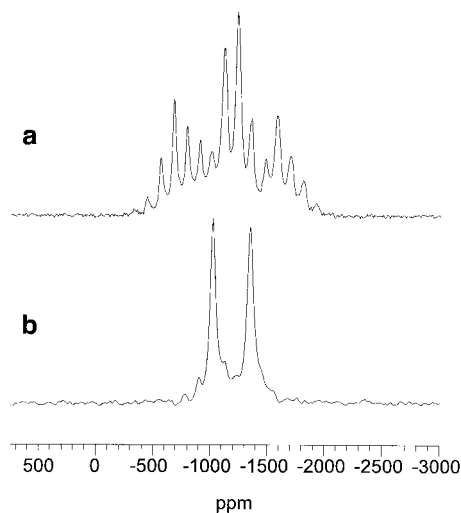

FIG. 4. (a) MAS and (b) isotropic ("infinite spinning rate") spectra of the $PbZrO_3$ sample, demonstrating the simplification achieved by the two-rotor-cycle 2D PASS experiment for samples with overlapping sidebands.

TABLE 2
Timings for π Pulses, in Units of Sample Revolutions, for Four-Rotor-Cycle PASS

Pitch ($\Theta/2\pi$)	$\theta_1/2\pi$	$\theta_2/2\pi$	$\theta_3/2\pi$	$\theta_4/2\pi$	$\theta_5/2\pi$[a]
0.0000	0.56307	1.31382	2.00000	2.56307	3.31382
0.0625	0.73629	1.40778	2.02130	2.74701	3.39721
0.1250	0.80411	1.47400	2.04547	2.82796	3.45238
0.1875	0.86239	1.53303	2.07523	2.90483	3.50024
0.2500	0.90729	1.58717	2.11202	2.97566	3.54353
0.3125	0.93986	1.63853	2.15459	3.04057	3.58466
0.3750	0.62538	1.10052	1.96387	2.68872	3.19999
0.4375	0.66686	1.15658	1.98300	2.73895	3.24567
0.5000	0.70979	1.20978	2.00000	2.79022	3.29022
0.5625	0.75433	1.26105	2.01700	2.84342	3.33314
0.6250	0.80001	1.31128	2.03613	2.89948	3.37462
0.6875	0.84541	1.36147	2.06014	2.95943	3.41534
0.7500	0.45647	1.02434	1.88798	2.41283	3.09271
0.8125	0.49976	1.09517	1.92477	2.46697	3.13761
0.8750	0.54762	1.17204	1.95453	2.52600	3.19589
0.9375	0.60279	1.25299	1.97870	2.59222	3.26372

[a] For shifted-echo detection, one or more additional rotor cycles can be inserted prior to and after this delay, as shown in Fig. 1.

tained here is most likely due to the contribution of the strong central sidebands, which are near the center of the probe bandwidth. Due to the wide chemical shift ranges found in ^{207}Pb NMR, it may not be possible to acquire accurate quantitative data for a sample with a single 2D PASS (or static or MAS) experiment.

Despite these issues, the separation of interactions by 2D PASS is clearly useful for assigning chemical shifts in ^{207}Pb NMR, as the anisotropic dimension serves to increase site resolution and identification in the isotropic dimension, while sideband overlap is avoided. This utility is magnified by the intended application of 2D PASS to amorphous samples, where a distribution of chemical shift tensor values would make exact fitting of such information difficult by any method.

A Four-Rotor-Cycle, Composite π Pulse 2D PASS Experiment

In cases of lead samples with a longer T_2 relaxation time, the sharper peaks can lead to an additional problem that can also be solved by multiple-rotor-cycle 2D PASS. RF field (B_1) inhomogeneity and off-resonance effects cause the effective π pulse width and nutation axis to vary across the sample, which leads to an additional undesired modulation of peaks by the 2D PASS sequence. The problem is especially severe for strong, sharp, off-resonance peaks. Using the full 243-step phase cycle can reduce this problem. However, its use is unreasonable for many ^{207}Pb-containing samples with longer T_1 relaxation times. The use of composite π pulses (31) with a suitable multiple-rotor-cycle 2D PASS experiment can be a good compromise in these situations.

As an example, a test sample with a 1:2 molar ratio of lead (II) nitrate (Pb(NO$_3$)$_2$) to lead sulfate (PbSO$_4$) was prepared. Both of these materials have T_1 values in the vicinity of 20 s, and both show a smaller CSA compared to the lead zirconate. The number of sidebands obtained from this mixture suggested an 8-kHz spinning speed for the 2D PASS experiment. In order to fit the longer composite pulses into a sequence at this spinning speed, a four-rotor-cycle 2D PASS sequence was necessary. The pulse timings for this sequence, solved for $\theta_T = 8\pi$, are given in Table 2. The spectra obtained with the four-rotor-cycle sequence, with and without composite pulses, are illustrated in Fig. 5. In the spectrum shown in Fig. 5a, a simple empirical phase cycle was employed, which consisted of a simple ($x, -x$) sequence of phase shifts for the five π pulses (to compensate for pulse width errors) combined with a cycle to suppress artifacts of the quadrature detection. The full 243-step cycle was not employed, as the experiment would have then required a total time of nearly 87 h to complete the phase cycle for each pitch. In Fig. 5a, large artifacts are visible running parallel to the F_1 dimension and make interpretation of the spectrum a potential problem.

In Fig. 5b, an improvement in spectral clarity is realized by use of composite π pulses. The π pulses were replaced with the composite pulse train $(\pi/2)_{\phi_1}-\pi_{\phi_2}-(\pi/2)_{\phi_1}$, where the ϕ values are the phases of the pulses, discussed below. This composite
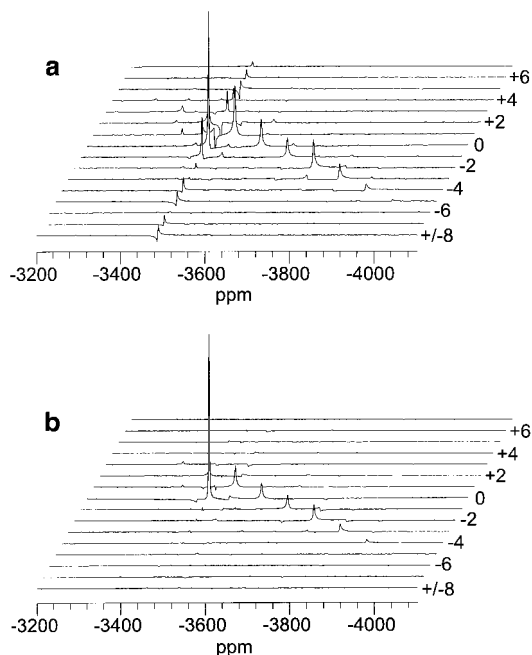

FIG. 5. (a) Results of a 16-pitch, four-rotor-cycle 2D PASS experiment on the mixture of Pb(NO$_3$)$_2$ and PbSO$_4$. (b) Results of a composite pulse version of the same sequence on the same sample. Both experiments were performed at a spinning speed of 8 kHz, with a π pulse duration of 7.0 μs and a recycle delay of 70 s. For both data sets, 40 acquisitions were performed at each pitch, requiring 12 h of experimental time. The phase cycle and composite pulses used in the experiments are discussed in the text.

TABLE 3
Phase Cycling Scheme Used in the Composite 2D PASS Experiment

$\pi/2$ pulse and receiver	Composite π pulses (ϕ_1, ϕ_2, ϕ_1)				
x	−y, x, −y	y, −x, y	−x, y, −x	x, −y, x	−y, x, −y
y	x, y, x	−x, −y, −x	y, x, y	−y, −x, −y	x, y, x
−x	y, x, y	−y, −x, −y	x, y, x	−x, −y, −x	y, x, y
−y	−x, y, −x	x, −y, x	−y, x, −y	y, −x, y	−x, y, −x

pulse train is designed primarily to suppress B_1 inhomogeneity problems, while also reducing off-resonance effects, and has been employed in both inversion and spin-echo (transverse) applications (*44*). An empirical phase cycle developed by Hagemeyer *et al.* (*32*) was used to enhance the artifact suppression of the sequence. Their phase cycle was extended by one additional composite pulse, and is reproduced in Table 3. In spin-echo situations, the composite pulse used here has been shown to introduce a phase shift in the magnetization related to errors in π pulse measurement (*44*), but this small effect cancels out for the first four composite pulses. It might lead to a phase shift after the fifth pulse, but this can be suppressed by use of accurate π pulse widths and normal phase correction.

The combination of phase cycling and composite pulses results in an improved spectrum that required only 12 h, saving time and improving artifact suppression over the other possible phase cycles. The full 243-step phase cycle could be combined with composite pulses in samples with shorter T_1 relaxation times. The major drawback to the four-rotor-cycle composite experiment is the loss of signal that would be observed in samples with shorter T_2 values, especially if the additional shifted-echo extension is used for samples with broader lines. This long sequence, requiring a total of six rotor periods, would not be amenable to many lead samples of interest. An additional problem is the increase in the total number of pulses from 6 to 16, even using the simplest composite pulse. If more sophisticated composite pulses are used, the situation could worsen. In practice, we have found that samples like lead zirconate are best analyzed by the shortest possible multiple-rotor-cycle experiment, even if regular π pulses are used (as was demonstrated above). However, for samples that have long T_2 values, such as metal–organic precursors to perovskite-phase materials (*27, 28*), composite pulses are a useful option.

CONCLUSION

Multiple-rotor-cycle versions of the 2D PASS experiment have been presented and demonstrated on ^{207}Pb-containing samples. The sequences reduce RF power requirements at higher spinning speeds, making the experiment technically feasible for many materials with larger chemical shift anisotropy. The utility of the 2D PASS method as an isotropic/anisotropic correlation experiment has already been demonstrated for lead phosphate glasses (*12*). Multiple-rotor-cycle

versions should enable further ^{207}Pb investigations of other glass systems, such as the lead borosilicate glasses (*21*). Many of these systems have only been studied by static ^{207}Pb NMR techniques, or have not been examined by NMR at all. The wide ranges of static fields and spinning speeds available in many laboratories, combined with PASS sequences designed for different spinning speed ranges, should also make 2D PASS applicable to other nuclei (such as ^{31}P) in amorphous samples. The use of multiple-rotor-cycle 2D PASS also allows for incorporation of longer composite pulses that greatly reduce spectral artifacts. This may have some use in applications to lead-containing perovskites and their precursors (*27, 28*).

ACKNOWLEDGMENTS

REFERENCES

1. I. J. Lowe, *Phys. Rev. Lett.* **2**, 285 (1959).
2. E. R. Andrew, A. Bradbury, and R. G. Eades, *Nature* **183**, 1802 (1958).
3. C. P. Slichter, "Principles of Magnetic Resonance," 3rd ed., Springer-Verlag, Heidelburg (1996).
4. M. M. Maricq and J. S. Waugh, *J. Chem. Phys.* **70**, 3300 (1979).
5. J. Herzfeld and A. E. Berger, *J. Chem. Phys.* **73**, 6021 (1980).
6. W. T. Dixon, *J. Chem. Phys.* **77**, 1800 (1982).
7. O. N. Antzutkin, S. C. Shekar, and M. H. Levitt, *J. Magn. Reson. A* **115**, 7 (1995).
8. J. J. Titman, S. F. de Lacroix, and H. W. Spiess, *J. Chem. Phys.* **98**, 3816 (1993).
9. Z. Song, O. N. Antzutkin, A. Rupprecht, and M. H. Levitt, *Chem. Phys. Lett.* **253**, 349 (1996).
10. B. Effey, J. A. Butcher, and R. L. Cappelletti, *J. Magn. Reson.* **132**, 266 (1998).
11. O. N. Antzutkin, Y. K. Lee, and M. H. Levitt, *J. Magn. Reson.* **135**, 144 (1998).
12. F. Fayon, C. Bessada, A. Douy, and D. Massiot, *J. Magn. Reson.* **137**, 116 (1999).
13. K. S. Kim and P. J. Bray, *J. Magn. Reson.* **16**, 334 (1974).
14. A. Nolle, *Z. Naturforsch. A* **32**, 964 (1977).

15. C. A. Fyfe, G. C. Gobbi, J. S. Hartman, R. E. Lenkinski, J. H. O'Brien, E. R. Beange, and M. A. R. Smith, *J. Magn. Reson.* **47,** 168 (1982).

16. F. Fayon, I. Farnan, C. Bessada, J. Coutures, D. Massiot, and J. P. Coutures, *J. Am. Chem. Soc.* **119,** 6837 (1997).

17. G. Neue, C. Dybowski, M. L. Smith, and D. H. Barich, *Solid State NMR* **3,** 115 (1994).

18. G. Neue, C. Dybowski, M. L. Smith, M. A. Hepp, and D. L. Perry, *Solid State NMR* **6,** 241 (1996).

19. Y. S. Kye and G. S. Harbison, *Inorg. Chem.* **37,** 6030 (1998).

20. C. Dybowski, M. L. Smith, M. A. Hepp, E. J. Gaffney, G. Neue, and D. L. Perry, *Appl. Spectrosc.* **52,** 426 (1998).

21. K. S. Kim, P. J. Bray, and S. Merrin, *J. Chem. Phys.* **64,** 4459 (1976).

22. T. Yoko, K. Tadanaga, F. Miyaji, and S. Sakka, *J. Non-Cryst. Solids* **150,** 192 (1992).

23. F. Fayon, C. Bessada, D. Massiot, I. Farnan, and J. P. Coutures, *J. Non-Cryst. Solids* **232–234,** 403 (1998).

24. F. Fayon, C. Landron, K. Sakurai, C. Bessada, and D. Massiot, *J. Non-Cryst. Solids* **243,** 39 (1999).

25. E. Sawaguchi, H. Maniwa, and S. Hoshino, *Phys. Rev.* **83,** 1078 (1951).

26. F. Jona, G. Shirane, F. Mazzi, and R. Pepinsky, *Phys. Rev.* **105,** 849 (1957).

27. C. D. Chandler, C. Roger, and M. J. Hampden-Smith, *Chem. Rev.* **93,** 1205 (1993).

28. A. D. Irwin, C. D. Chandler, R. Assink, and M. J. Hampden-Smith, *Inorg. Chem.* **33,** 1005 (1994).

29. D. J. Aurentz, F. G. Vogt, K. T. Mueller, and A. J. Benesi, *J. Magn. Reson.* **138,** 320 (1999).

30. D. Massiot, V. Montouillout, F. Fayon, P. Florian, and C. Bessada, *Chem. Phys. Lett.* **272,** 295 (1997).

31. M. H. Levitt, *Prog. NMR Spectrosc.* **18,** 61 (1986).

32. A. Hagemeyer, D. van der Puten, and H. W. Spiess, *J. Magn. Reson.* **92,** 628 (1991).

33. O. N. Antzutkin, Z. Song, X. Feng, and M. H. Levitt, *J. Chem. Phys.* **100,** 130 (1994).

34. M. H. Levitt, *J. Magn. Reson.* **82,** 427 (1989).

35. M. M. Maricq and J. S. Waugh, *J. Chem. Phys.* **70,** 3300 (1979).

36. S. Wolfram, "Mathematica: A System for Doing Mathematics by Computer," Addison–Wesley, Reading, MA (1996).

37. W. H. Press, B. P Flannery, S. A. Teukolsky, and W. T. Vetterling, "Numerical Recipes in C," 2nd ed., Cambridge Univ. Press, London (1995).

38. A. Bielecki and D. P. Burum, *J. Magn. Reson. A* **116,** 215 (1995).

39. L. C. M. van Gorkom, J. M. Hook, M. B. Logan, J. V. Hanna, and R. E. Wasylishen, *Magn. Reson. Chem.* **33,** 791 (1995).

40. G. Neue and C. Dybowski, *Solid State NMR* **7,** 333 (1997).

41. R. R. Ernst, G. Bodenhausen, and A. Wokaun, "Principles of Nuclear Magnetic Resonance in One and Two Dimensions," p. 203, Clarendon Press, Oxford (1987).

42. A. F. Wells, "Structural Inorganic Chemistry," 5th ed., Oxford Univ. Press, New York (1984).

43. G. L. Turner, K. A. Smith, R. J. Kirkpatrick, and E. Oldfield, *J. Magn. Reson.* **70,** 408 (1986).

44. M. H. Levitt and R. Freeman, *J. Magn. Reson.* **43,** 65 (1981).